Computers and Mathematics with Applications 75 (2018) 2538–2548

Contents lists available at ScienceDirect

Computers and Mathematics with Applications

journal homepage: www.elsevier.com/locate/camwa

N-solitons, breathers, lumps and rogue wave solutions to a (3+1)-dimensional nonlinear evolution equation

Yunfei Yue [a], Lili Huang [a], Yong Chen [a,b,*]

[a] Shanghai Key Laboratory of Trustworthy Computing, East China Normal University, Shanghai, 200062, China
[b] Department of Physics, Zhejiang Normal University, Jinhua, 321004, China

ARTICLE INFO

Article history:
Received 7 August 2017
Received in revised form 8 November 2017
Accepted 22 December 2017
Available online 1 February 2018

Keywords:
Hirota bilinear method
Kink soliton solution
Breather
Rogue wave

ABSTRACT

Based on Hirota bilinear method, N-solitons, breathers, lumps and rogue waves as exact solutions of the (3+1)-dimensional nonlinear evolution equation are obtained. The impacts of the parameters on these solutions are analyzed. The parameters can influence and control the phase shifts, propagation directions, shapes and energies for these solutions. The single-kink soliton solution and interactions of two and three-kink soliton overtaking collisions of the Hirota bilinear equation are investigated in different planes. The breathers in three dimensions possess different dynamics in different planes. Via a long wave limit of breathers with indefinitely large periods, rogue waves are obtained and localized in time. It is shown that the rogue wave possess a growing and decaying line profile that arises from a nonconstant background and then retreat back to the same nonconstant background again. The results can be used to illustrate the interactions of water waves in shallow water. Moreover, figures are given out to show the properties of the explicit analytic solutions.

1. Introduction

With the rapid development of science and computer technology, the human cognition and research object gradually went from linear models to nonlinear models. As one of the three branches of nonlinear science, the theory of solitons has become an important research field of nonlinear science and has aroused great interests. These nonlinear models are applied to many fields, such as fluid, plasma, nonlinear optics, biologic nerve propagation, atmospheric science, marine science and so on. To find exact solutions of nonlinear systems is a difficult and tedious but very important and meaningful work. So far, several effective methods have been established by mathematicians and physicists to obtain exact solutions of soliton equations, such as the Inverse Scattering transformation (IST) [1], Darboux transformation (DT) [2,3], Painlevé analysis [4,5], Hirota bilinear method [6,7], Bäcklund transformation (BT) [8], Lie symmetry method [9–11] and so on.

Recently, the study of breathers, lumps and rogue waves has attracted more and more attention in the nonlinear fields. Solitons, breathers, lumps, and rogue waves are different types of nonlinear localized waves and are key objects in nonlinear physical systems such as nonlinear optics, bio-physics, plasmas, cold atoms, and Bose–Einstein condensates. Solitons are the stable waves, while rogue waves and breathers are localized structures on a background with unstable characteristics. Breathers [12–16] are regarded as the crucial prototypes to explain rogue wave phenomena and are the localized breathing waves with a periodic profile in a certain direction. As a kind of rational function solutions, lumps [17–22] are localized in all directions in the space, lump-type [23,24] solutions are localized in almost all directions in the space. Rogue waves

* Corresponding author at: Shanghai Key Laboratory of Trustworthy Computing, East China Normal University, Shanghai, 200062, China.
E-mail address: ychen@sei.ecnu.edu.cn (Y. Chen).

https://doi.org/10.1016/j.camwa.2017.12.022
0898-1221/

[25–33] are localized in both space and time, and appear from nowhere and disappear without a trace [34], have taken the responsibility for numerous marine disasters.

In this paper, we focus on N-solitons, breathers, lumps and rogue wave solutions of the following $(3+1)$-dimensional nonlinear evolution equation (NLEE) [35–39]

$$u_{yt} - u_{xxxy} - 3(u_x u_y)_x - 3u_{xx} + 3u_{zz} = 0, \tag{1}$$

which was first proposed in [36] by using a multivariate polynomial. Based on the bilinear form, Lü and Ma [37] have obtained lump solutions by two types of dimensional reductions and given the sufficient and necessary conditions to guarantee analyticity and rational localization of the solutions. For the $(3+1)$-dimensional NLEE (1), only multiple wave solutions, lump solutions have been investigated. It is important to study other rational solutions to Eq. (1). Via the method used in [40], we will report some new localized wave solutions of the $(3+1)$-dimensional NLEE.

The paper is organized as follows. In Section 2, based on Hirota bilinear method, one, two and three-soliton solutions are obtained, even derived the form of N-soliton solution. In Section 3, upon choosing appropriate parameters on the two-soliton solution, the line breathers are derived and their dynamical behaviors are shown under different planes and parameters. In Section 4, via a long wave limit of breathers, localized rational solutions are proposed. By modifying the internal parameters, the line rogue waves and the lumps are derived from the rational solutions. The last section contains a short summary and discussion.

2. The soliton solutions

By using a dependent variable transformation

$$u = 2[\ln f(x, y, z, t)]_x = 2\frac{f_x(x, y, z, t)}{f(x, y, z, t)}, \tag{2}$$

Eq. (1) can be mapped into

$$(D_t D_y - D_x^3 D_y - 3D_x^2 + 3D_z^2)(f \cdot f) = 0, \tag{3}$$

that is

$$2[ff_{ty} - f_y f_t + f_{xxx} f_y - ff_{xxxy} + 3f_x f_{xxy} - 3f_{xx} f_{xy} - 3(ff_{xx} - f_x^2) + 3(ff_{zz} - f_z^2)] = 0, \tag{4}$$

where $f = f(x, y, z, t)$, and the derivatives $D_t D_y$, $D_x^3 D_y$, D_x^2 and D_z^2 are all the bilinear derivative operators [6] defined by

$$D_x^\alpha D_y^\beta D_z^\gamma D_t^\delta (f \cdot g) = (\frac{\partial}{\partial x} - \frac{\partial}{\partial x'})^\alpha (\frac{\partial}{\partial y} - \frac{\partial}{\partial y'})^\beta (\frac{\partial}{\partial z} - \frac{\partial}{\partial z'})^\gamma (\frac{\partial}{\partial t} - \frac{\partial}{\partial t'})^\delta f(x, y, z, t) g(x', y', z', t')|_{x'=x, y'=y, z'=z, t'=t}. \tag{5}$$

It is clear that if f solves Eq. (4), then $u = u(x, y, z, t)$ is a solution of Eq. (1) through the transformation (2).

2.1. The 1-soliton solution

To search for one-soliton solution of the $(3+1)$-dimensional NLEE in Eq. (1), assuming f in the following form

$$f = 1 + e^{\eta_1}, \tag{6}$$

where

$$\eta_1 = k_1(x + p_1 y + q_1 z + \omega_1 t) + \eta_1^0, \tag{7}$$

with k_1, p_1, q_1, and η_1^0 are arbitrary constants.

Substituting Eq. (6) with Eq. (7) into Eq. (3), and making the coefficients of all exponential functions to zero, we can obtain

$$\omega_1 = k_1^2 + \frac{3(1 - q_1^2)}{p_1}. \tag{8}$$

Then substituting Eqs. (6)–(8) into Eq. (2), the one-soliton solution of Eq. (1) can be obtained.

If setting $k_1 = 2, p_1 = 1, q_1 = 1, \eta_1^0 = 0$, we can obtain one-kink soliton solution and give the wave shape in different planes, which is shown in Fig. 1.

2.2. The 2-soliton solution

To search for two-soliton solution of the $(3+1)$-dimensional NLEE in Eq. (1), assuming f in the following form

$$f = 1 + e^{\eta_1} + e^{\eta_2} + A_{12} e^{\eta_1 + \eta_2}, \tag{9}$$

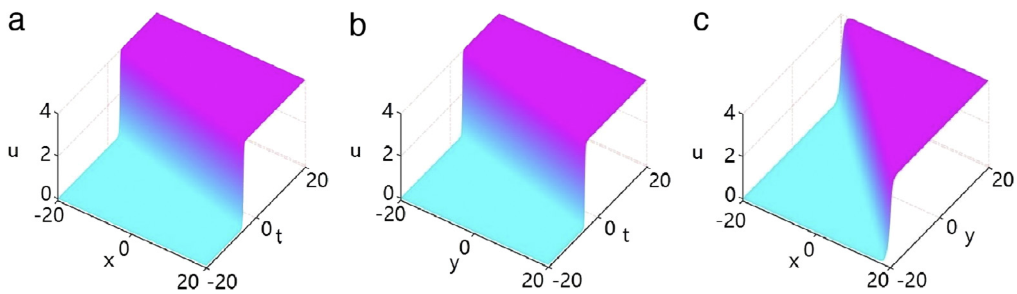

Fig. 1. The one-kink soliton solution for Eq. (1) by choosing suitable parameters: $k_1 = 2, p_1 = 1, q_1 = 1, \eta_1^0 = 0$. (a) $y = 0, z = 0$; (b) $x = 0, z = 0$; (c) $z = 0, t = 0$.

where

$$\eta_i = k_i(x + p_i y + q_i z + \omega_i t) + \eta_i^0 \ (i = 1, 2), \tag{10}$$

with k_i, p_i, q_i and η_i^0 are arbitrary constants.

Substituting Eq. (9) with Eq. (10) into Eq. (3), and making the coefficients of all exponential functions to zero, we can obtain

$$\begin{aligned} \omega_i &= k_i^2 + \frac{3(1-q_i^2)}{p_i} \ (i = 1, 2), \\ A_{12} &= \frac{p_1p_2(k_1 - k_2)(k_1p_1 - k_2p_2) + (p_1q_2 - p_2q_1)^2 - (p_1 - p_2)^2}{p_1p_2(k_1 + k_2)(k_1p_1 + k_2p_2) + (p_1q_2 - p_2q_1)^2 - (p_1 - p_2)^2}. \end{aligned} \tag{11}$$

Then substituting Eqs. (9)–(11) into Eq. (2), the two-soliton solution of Eq. (1) can be obtained.

If setting $k_1 = 2, p_1 = 1, q_1 = 2, k_2 = 3, p_2 = 2, q_2 = 1$, and $\eta_1^0 = \eta_2^0 = 0$, we can obtain a two-kink solution and give the wave shape in different planes, which is shown in Fig. 2.

2.3. The 3-soliton solution

For three-soliton solution of the (3 + 1)-dimensional NLEE in Eq. (1), assuming f in the following form

$$f = 1 + e^{\eta_1} + e^{\eta_2} + e^{\eta_3} + A_{12}e^{\eta_1+\eta_2} + A_{23}e^{\eta_2+\eta_3} + A_{13}e^{\eta_1+\eta_3} + A_{123}e^{\eta_1+\eta_2+\eta_3}, \tag{12}$$

where

$$\eta_i = k_i(x + p_i y + q_i z + \omega_i t) + \eta_i^0 \ (i = 1, 2, 3), \tag{13}$$

with k_i, p_i, q_i and η_i^0 are arbitrary constants.

Based on above method, substituting Eq. (12) with Eq. (13) into Eq. (3), we can obtain

$$\begin{aligned} \omega_i &= k_i^2 + \frac{3(1-q_i^2)}{p_i}, \\ A_{ij} &= \frac{p_ip_j(k_i - k_j)(k_ip_i - k_jp_j) + (p_iq_j - p_jq_i)^2 - (p_i - p_j)^2}{p_ip_j(k_i + k_j)(k_ip_i + k_jp_j) + (p_iq_j - p_jq_i)^2 - (p_i - p_j)^2} \ (i = 1, 2, 3), \\ A_{12}A_{23}A_{13} &= A_{123}. \end{aligned} \tag{14}$$

Then substituting Eqs. (12)–(14) into Eq. (2), the three-soliton solution of Eq. (1) can be obtained.

If setting $k_1 = 1.6, p_1 = 1.2, q_1 = 2, k_2 = 2.1, p_2 = 2.3, q_2 = 1, k_3 = 1.3, p_3 = 3.3, q_3 = 2$ and $\eta_1^0 = \eta_2^0 = \eta_3^0 = 0$, we can obtain a three-kink soliton solution, which is shown in Fig. 3.

It is visually shown that the collisions are elastic and the propagation situations of solitary waves can be seen via the above four pictures. Figs. 1–3 show the one-kink soliton, two-kink soliton, and three-kink soliton, respectively, by choosing suitable parameters. The shapes and speeds of the solitons have no change, but the phases may have a change after the collisions. The small-amplitude solitons overtake the large-amplitude ones, which can be seen in Fig. 4.

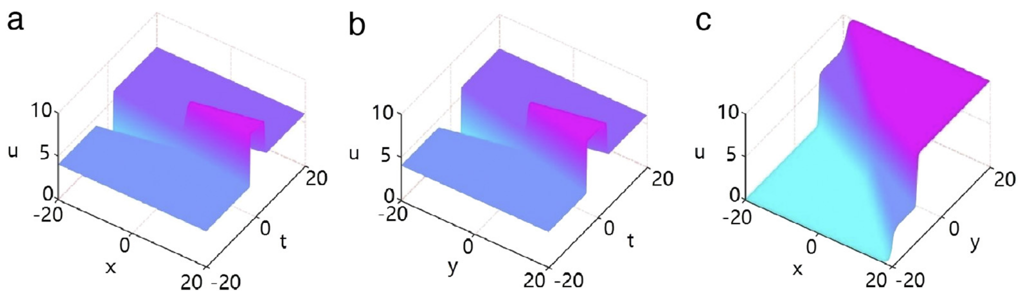

Fig. 2. The two-kink soliton solution for Eq. (1) by choosing suitable parameters: $k_1 = 2, p_1 = 1, q_1 = 2, k_2 = 3, p_2 = 2, q_2 = 1, \eta_1^0 = 0, \eta_2^0 = 0$. (a) $y = 0$, $z = 0$; (b) $x = 0, z = 0$; (c) $z = 0, t = 0$.

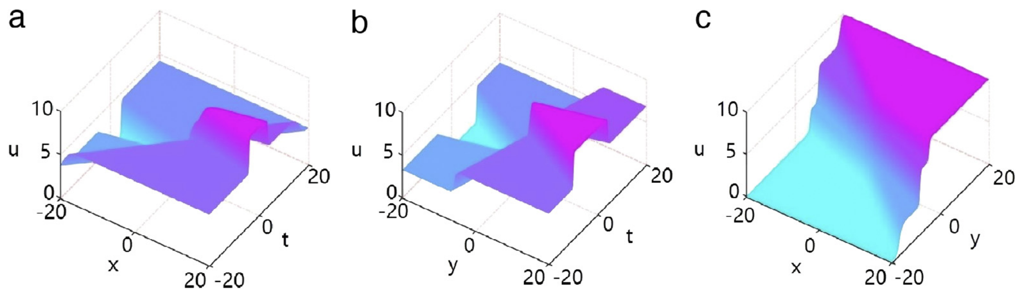

Fig. 3. The three-kink soliton solution for Eq. (1) by choosing suitable parameters: $k_1 = 1.6, p_1 = 1.2, q_1 = 2, k_2 = 2.1, p_2 = 2.3, q_2 = 1, k_3 = 1.3$, $p_3 = 3.3, q_3 = 2, \eta_1^0 = 0, \eta_2^0 = 0, \eta_3^0 = 0$. (a) $y = 0, z = 0$; (b) $x = 0, z = 0$; (c) $z = 0, t = 0$.

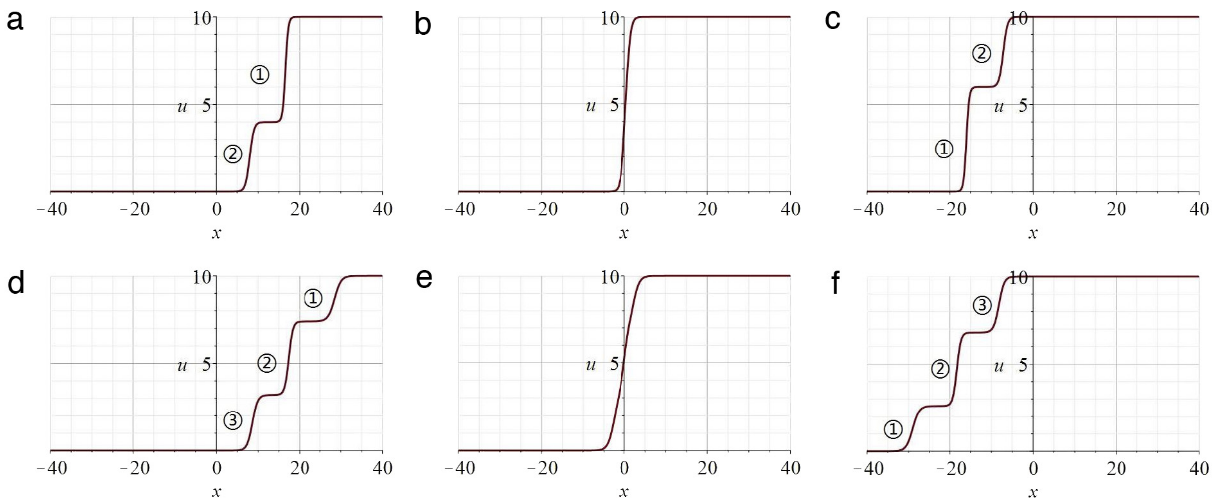

Fig. 4. Interaction of the soliton overtaking collision of $z = 0, t = 0, \eta_1^0 = 0, \eta_2^0 = 0, \eta_3^0 = 0$. (a), (b) and (c) Interaction of the two solutions overtaking collision of $k_1 = 2, p_1 = 1, q_1 = 2, k_2 = 3, p_2 = 2, q_2 = 1$ at $t = 0, y = -6, 0, 6$; (d), (e) and (f) Interaction of the three solutions overtaking collision of $k_1 = 1.6, p_1 = 1.2, q_1 = 2, k_2 = 2.1, p_2 = 2.3, q_2 = 1, k_3 = 1.3, p_3 = 3.3, q_3 = 2$ at $t = 0, y = -7.2, 0.8, 8.8$.

2.4. The N-soliton solution

Continuing the above process, the N-soliton solution of Eq. (1) can be deduced by the similar way. The function f meets the following form:

$$f = \sum_{\mu=0,1} \exp\Big(\sum_{i=1}^{N} \mu_i \eta_i + \sum_{1\le i<j}^{N} \mu_i \mu_j \ln(A_{ij})\Big), \tag{15}$$

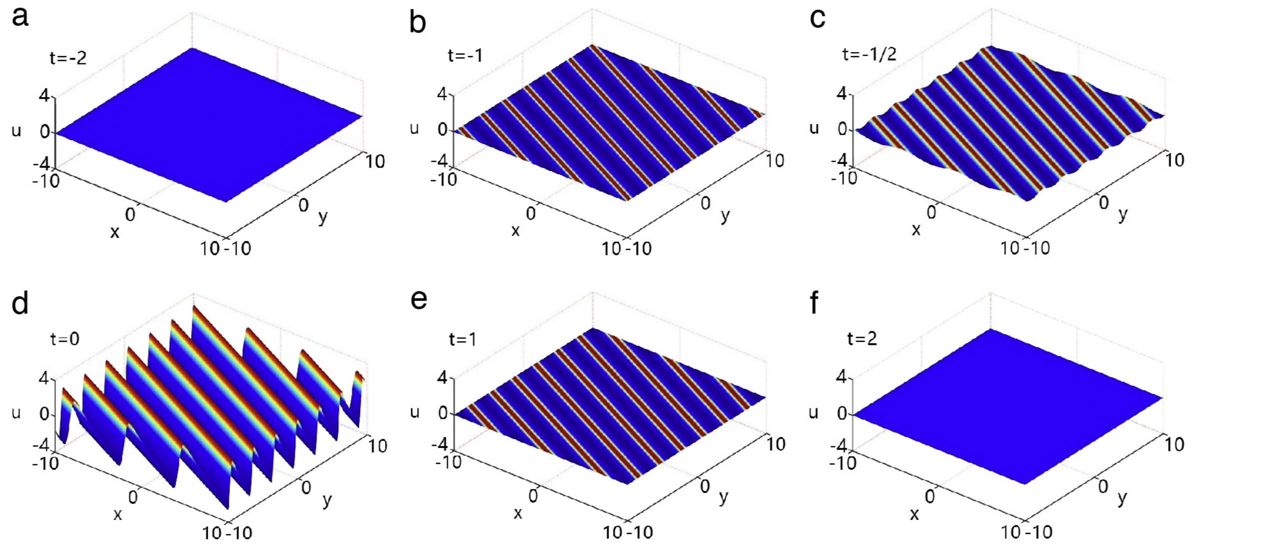

Fig. 5. The time evolution of line breathers of Eq. (1) in the (x, y) plane for parameters of Eq. (18) at $z = 0$.

where

$$\begin{aligned} \omega_i &= k_i^2 + \frac{3(1-q_i^2)}{p_i}, \quad \eta_i = k_i(x + p_i y + q_i z + \omega_i t) + \eta_i^0, \\ A_{ij} &= \frac{p_i p_j (k_i - k_j)(k_i p_i - k_j p_j) + (p_i q_j - p_j q_i)^2 - (p_i - p_j)^2}{p_i p_j (k_i + k_j)(k_i p_i + k_j p_j) + (p_i q_j - p_j q_i)^2 - (p_i - p_j)^2} \ (i = 1, 2, \ldots, N) \end{aligned} \tag{16}$$

with k_i, p_i, q_i and η_i^0 are arbitrary constants and $\sum_{\mu=0,1}$ is the summation that takes over all possible combinations of $\eta_i, \eta_j = 0, 1 (i, j = 1, 2, \ldots, N)$. Substituting Eq. (15) with (16) into Eq. (2), the N-soliton solution can be obtained.

3. The breather solutions

Based on the conditions of obtaining breathers mentioned in the previous works, an analytical expression for the breather solutions can be obtained by choosing suitable parameters on the two-soliton solution in Eq. (2), which has a similar form with the two-dimensional equations.

Now substituting the function f into the solution (2) of Eq. (1), line breathers can be obtained in the (x, y) plane, where the parameters in Eq. (2) need to satisfy the following conditions

$$k_1 = Ia_1, \ k_2 = -Ia_2, \ p_1 = b_1, \ p_2 = b_1, \ q_1 = a + Ik, \ q_2 = a - Ik. \tag{17}$$

For instance, setting parameters as follows

$$k_1 = k_2^* = I, \ p_1 = p_2 = 2, \ q_1 = q_2^* = 1 + 2I, \ \eta_1^0 = \eta_2^0 = 0, \tag{18}$$

the function f in Eq. (9) of u can be rewritten as

$$\begin{aligned} f &= 1 + 2\cosh(6t - 2z)\cos(x + 2y + z + 5t) + 2\sinh(6t - 2z)\cos(x + 2y + z + 5t) \\ &\quad + \frac{3}{2}\cosh(12t - 4z) + \frac{3}{2}\sinh(12t - 4z). \end{aligned} \tag{19}$$

Dynamical behaviors of corresponding solutions u can be obtained in the (x, y) along with the time evolution, which are shown in Fig. 5. Along with the time, these periodic line waves obviously start from the constant state and reach maximum amplitudes at $t = 0$, then gradually start to damp and finally return to the initial constant state. These periodic line waves remain parallel and independent of each other, but the changes of their behaviors are consistent along with the time. As the fundamental line rogue waves can be treated as a limited case of these period line waves, hereafter we refer to these periodic line waves as line breathers. If setting the same parameters in different planes, these breather solutions will display different behavior characteristics. By comparing Fig. 5 with Fig. 6, the above conclusions can be obtained. Just looking from Fig. 6, the breathers spread in the same direction, but have different number of waves in different planes. When choosing the (x, z) plane, switching the value of p_1 and q_1 in Eq. (18) and setting $k_1 = 2I$, it is worth pointing out that these periodic solutions also describe line breathers, which are shown in Fig. 7. From Figs. 5 and 7, it is not difficult to find that these periodic solutions have different periodic.

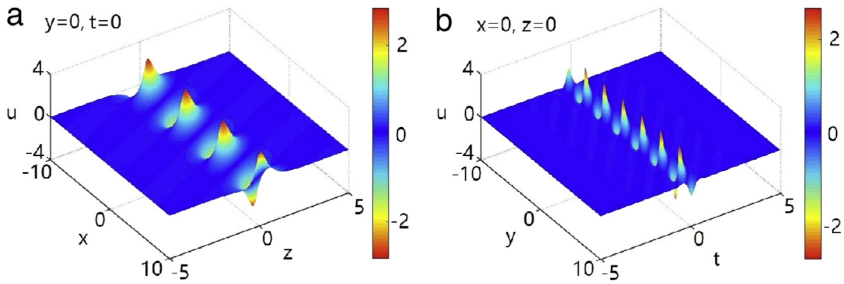

Fig. 6. Breathers of Eq. (1) in the (x, z) plane and the (y, z) plane for parameters of Eq. (18).

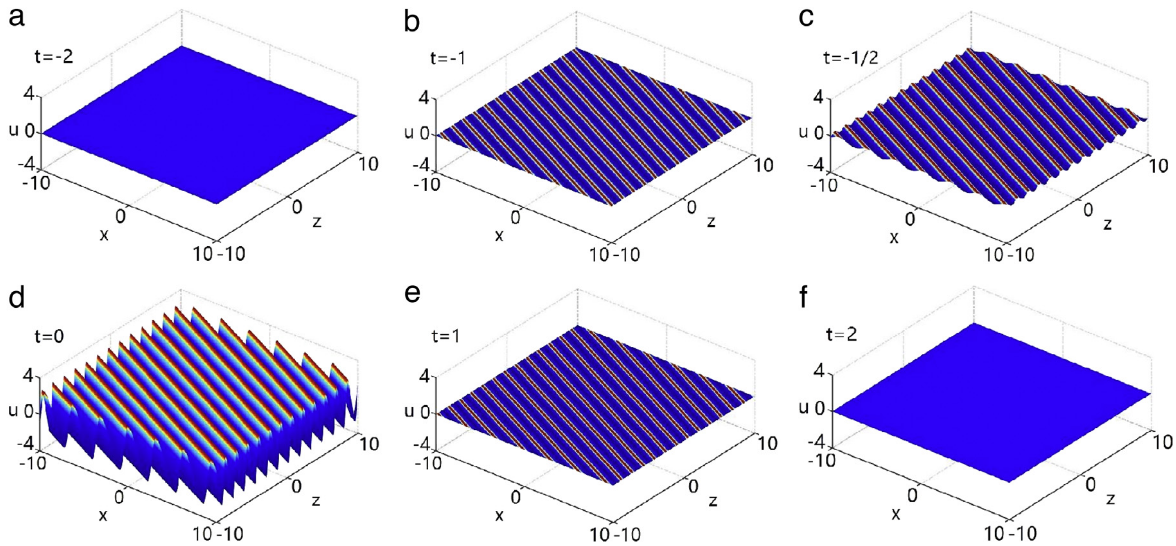

Fig. 7. The time evolution of line breathers of Eq. (1) in the (x, z) plane for parameters $k_1 = 2I,\ \ k_2 = -2I,\ \ p_1 = 1 - 2I,\ \ p_2 = 1 + 2I,\ \ q_1 = 2,\ \ q_2 = 2$ and $y = 0$.

4. The lump solution and rogue wave solution

In order to obtain the rogue waves, a long wave limit of function f in Eq. (9) must be taken. Setting parameters

$$k_1 = l_1\epsilon,\ \ k_2 = l_2\epsilon,\ \ \eta_1^0 = \eta_2^{0*} = I\pi, \tag{20}$$

in Eq. (9) and taking the limit as $\epsilon \to 0$, the function f can be rewritten as

$$f = (\theta_1\theta_2 + \theta_0)l_1l_2\epsilon^2 + O(\epsilon^3), \tag{21}$$

where

$$\begin{aligned} \theta_0 &= \frac{2p_1p_2(p_1+p_2)}{(p_1-p_2)^2-(p_1q_2-p_2q_1)^2}, \\ \theta_i &= \frac{p_i^2y + p_iq_iz - 3q_i^2t + p_ix + 3t}{p_i} \quad (i = 1, 2). \end{aligned} \tag{22}$$

Substituting Eq. (21) with Eq. (22) into Eq. (2), the solution u can be expressed as

$$u = \frac{2(\theta_1+\theta_2)}{\theta_1\theta_2+\theta_0}. \tag{23}$$

Setting

$$p_2 = p_1^*,\ \ q_2 = q_1^*, \tag{24}$$

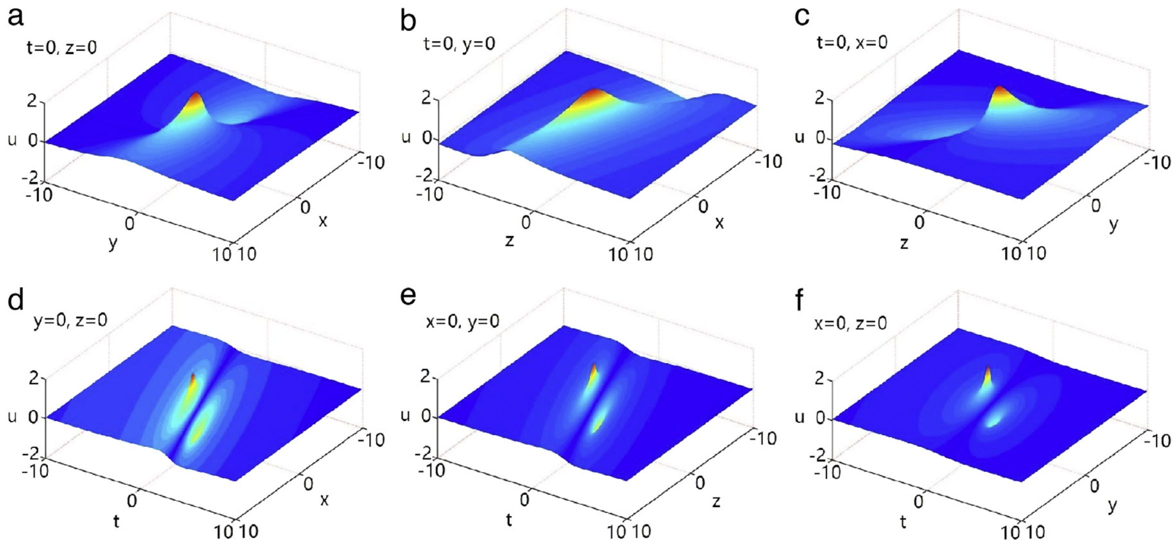

Fig. 8. Lump solutions (23) of Eq. (1) in different planes for parameters $p_1 = 1 + 2I$, $p_2 = 1 - 2I$, $q_1 = 2 + I$, $q_2 = 2 - I$.

the following conditions $\theta_2 = \theta_1^*$ and $\theta_0 > 0$ can be obtained. So the solution u in Eq. (23) is nonsingular. Moreover, this solution has two different dynamical behaviors in each plane. Next, these two different dynamical behaviors are given in the (x, y) plane as an example.

Setting $p_1 = a_1 + Ib_1$, $q_1 = a_2 + Ib_2$, and a_1, a_2, b_1, b_2 are all real constants.

Case 1. Lump solution

When $a_1 \neq 0$, along a trajectory defined by $[x(t), y(t)]$, where

$$\begin{aligned} &x + \frac{(3 - 3a_2^2 + 3b_2^2)t}{a_1} + \frac{(a_1^2 - b_1^2)y}{a_1} + \frac{(a_1a_2 - b_1b_2)z}{a_1} - \sqrt{\frac{a_1(a_1^2 + b_1^2)}{(a_1b_2 - a_2b_1 + b_1)(a_1b_2 - a_2b_1 - b_1)}} = 0, \\ &b_1y + b_2z - \frac{3(2a_1a_2b_2 - a_2^2b_1 + b_1b_2^2 + b_1)t}{a_1^2 + b_1^2} = 0, \end{aligned} \tag{25}$$

the solution u in Eq. (23) is a constant. Moreover, $u \to 0$ when (x, y) goes to infinity at any given (t, z). So it can be found that these rational solutions keep moving in permanent lumps status on the kink backgrounds. These solutions are rationally localized in all directions in the space.

If choosing parameters as above in Eq. (24), lumps (i.e., one global maximum point and two global minimum points) in Eq. (1) can arise. The dynamic behaviors of lump solutions in different planes are visually shown in Fig. 8. It should be pointed out that choosing any surface to be projected, the obtained solutions are lump solutions in $\mathbb{R}^3$ in above figures, while these solutions are lump-type solutions in $\mathbb{R}^4$.

Case 2. Rogue wave solution

When $b_1 = 0$ (i.e., p_1 is real), the solution u in Eq. (23) is line rogue wave in the (x, y) plane, whose amplitude changes along the time, see Fig. 9. There are obvious differences between line solitons and line rogue waves during their propagation. When $t = 0$, the solution u in Eq. (23) can reach a higher amplitude in the (x, y) plane, but when $|t| \gg 0$, it returns to the initial kink state. This solution is a rational growing and decaying mode. Obviously, these solutions are located in time and are called line rogue waves in previous works.

At the same time, line rogue wave solutions can be also obtained by choosing suitable parameters in the (x, z) and (y, z) planes. When $b_2 = 0$, the solution u in Eq. (23) is line rogue wave in the (x, z) plane. Setting $p_1 = 1 - 2I$, $q_1 = 2$, the corresponding line rogue wave solution can be obtained in the (x, z) plane, which is illustrated in Fig. 10. When $a_2 = 0$, $b_2 = 0$, line rogue wave solution can be obtained in the (y, z) plane. Setting $p_1 = -1 + I$, $p_2 = -1 - I$, the corresponding line rogue wave solution can be obtained in the (y, z) plane, which is plotted in Fig. 11.

It should be point out that lump solutions can be also obtained in the (x, z) and (y, z) planes under the above same parameters, whose amplitudes unchange, but positions change along the time. Their dynamic phenomena are illustrated in Fig. 12 and Fig. 13 respectively.

Through the above analysis, it seems impossible that rogue wave phenomena appear in different planes under the same parameters, but rogue wave phenomena can appear in different planes by choosing appropriate parameters. Based on the method used in this paper, it is not possible to obtain the general rogue wave solution of Eq. (23), while the line rogue wave

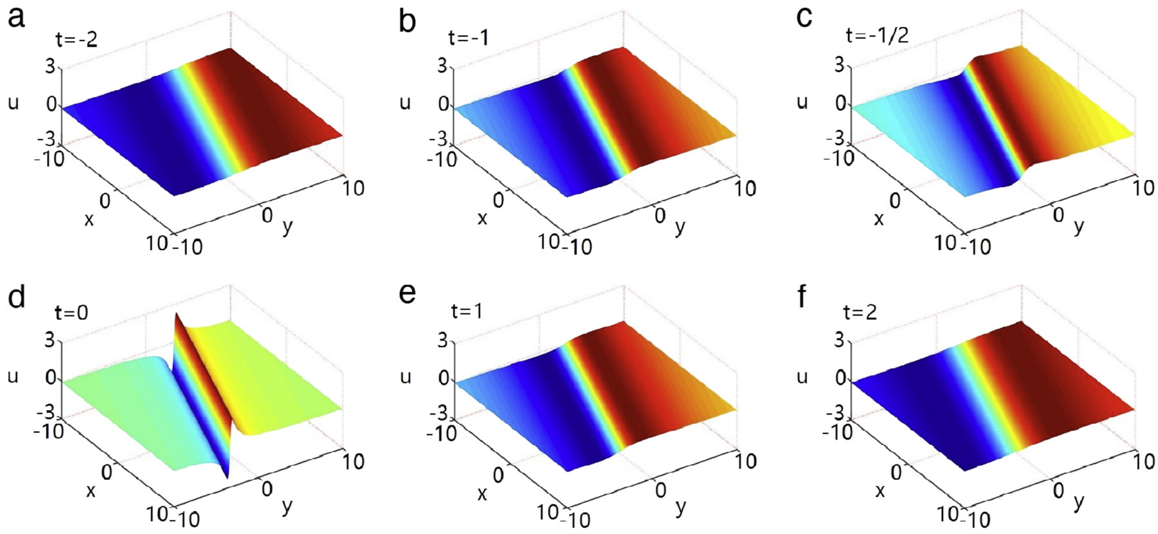

Fig. 9. The time evolution of line rogue waves (23) of Eq. (1) in the (x, y) plane for parameters $p_1 = 3$, $p_2 = 3$, $q_1 = 2 + 2I$, $q_2 = 2 - 2I$ at $z = 0$.

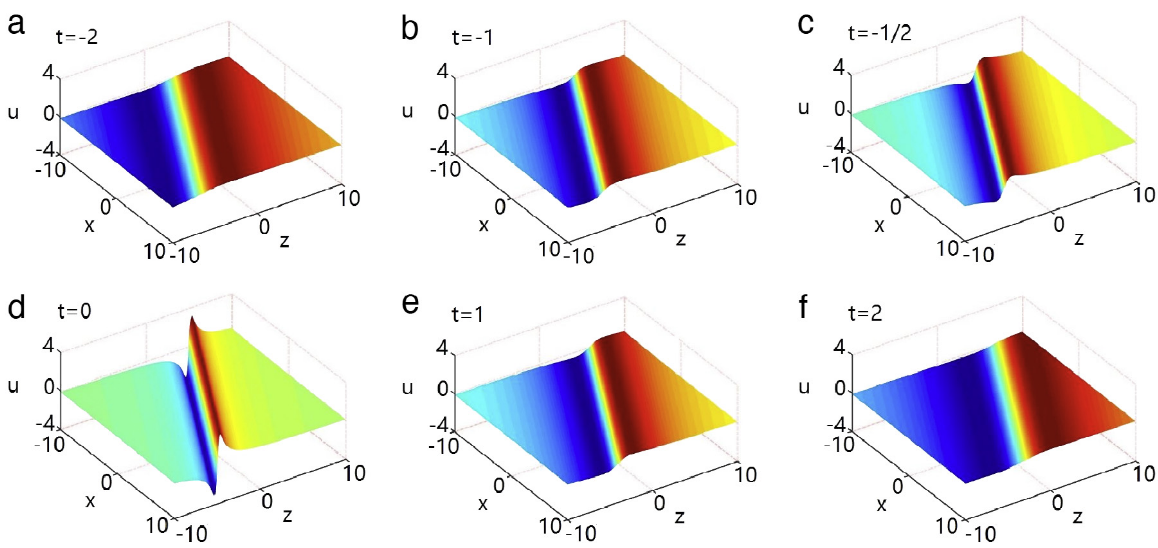

Fig. 10. The time evolution of line rogue waves (23) of Eq. (1) in the (x, z) plane for parameters $p_1 = 1 - 2I$, $p_2 = 1 + 2I$, $q_1 = 2$, $q_2 = 2$ at $y = 0$.

solution can be derived. In the next study, we expect to obtain the general rogue wave solutions by modifying the above method.

5. Summary and discussions

In summary, the kink soliton solutions of the $(3+1)$-dimensional NLEE are obtained based on the Hirota bilinear method. In this paper, one to three soliton solutions are given. The form of N-soliton solution is even deduced in accordance with the above soliton solutions. They all show the kink soliton form. Their collisions are elastic, that is, the shapes, amplitudes, widths, and velocities keep invariable during the propagation, just the phases have a change. On the basis of two-soliton solution, line breathers are obtained by setting specific parameters. The line breather starts from the constant background and reaches maximum amplitude at $t = 0$, then gradually starts to damp and finally returns to the initial constant state. These line breathers remain parallel and independent of each other. By taking limitation, two different dynamical behavioral solutions can be obtained, which are lump solution and rogue wave solution. It is worthy to point out that they are lump-type [23,24]

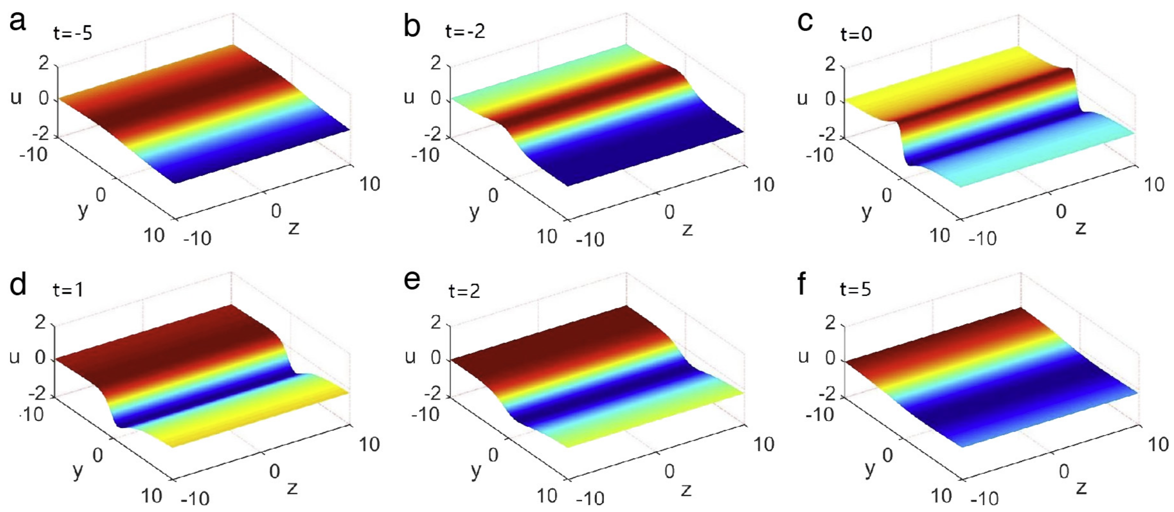

Fig. 11. The time evolution of line rogue waves (23) of Eq. (1) in the (y, z) plane for parameters $p_1 = -1 + I$, $p_2 = -1 - I$ at $x = 0$.

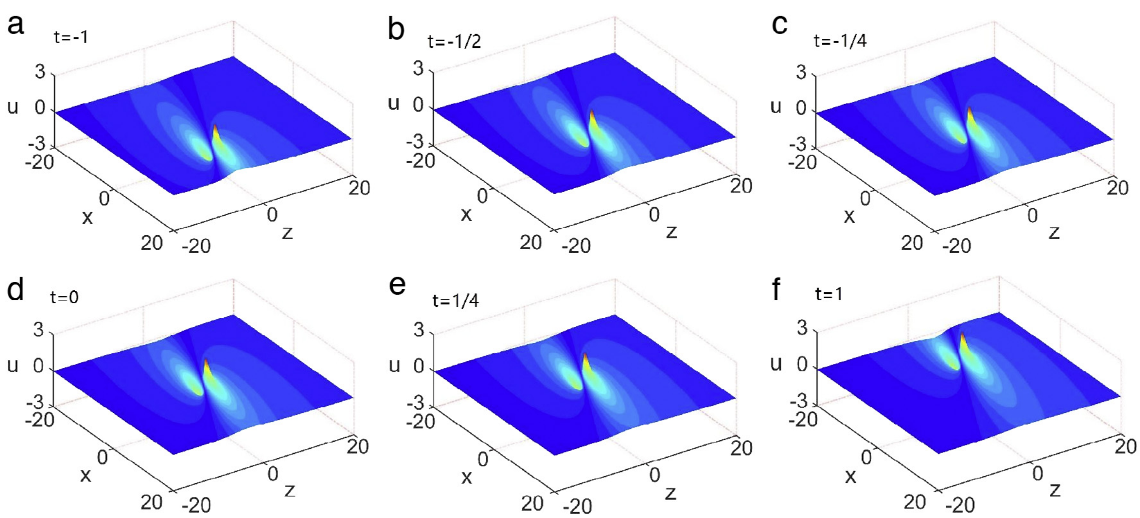

Fig. 12. The time evolution of lump solutions (23) of Eq. (1) in the (x, z) plane for parameters $p_1 = 3$, $p_2 = 3$, $q_1 = 2 + 2I$, $q_2 = 2 - 2I$ at $y = 0$.

solutions in $\mathbb{R}^4$. They attract recent attention in describing nonlinear wave phenomena in oceanography and nonlinear optics. Dynamical behaviors of lump solutions are visually shown in different planes. Line rogue waves are rational growing and decaying modes and located in time. These effective methods used in this paper provide a direct and powerful mathematical tool to derive exact localized wave solutions of other nonlinear models, which can be helpful to study nonlinear evolution equations in mathematical physics and engineering. It is worthy of further exploration to apply numerical simulation method to the above theoretical solutions in the future. Based on the above similar method, the interaction solutions can be also obtained, whose relevant results will be reported in a separate work.

Acknowledgments

We would like to express our sincere thanks to S.Y. Lou, E.G. Fan, Z.Y. Yan, B. Li and other members of our discussion group for their valuable comments. The project is supported by the Global Change Research Program of China (No. 2015CB953904), National Natural Science Foundation of China (Nos. 11675054 and 11435005), Outstanding doctoral dissertation cultivation plan of action (No. YB2016039), and Shanghai Collaborative Innovation Center of Trustworthy Software for Internet of Things (No. ZF1213).

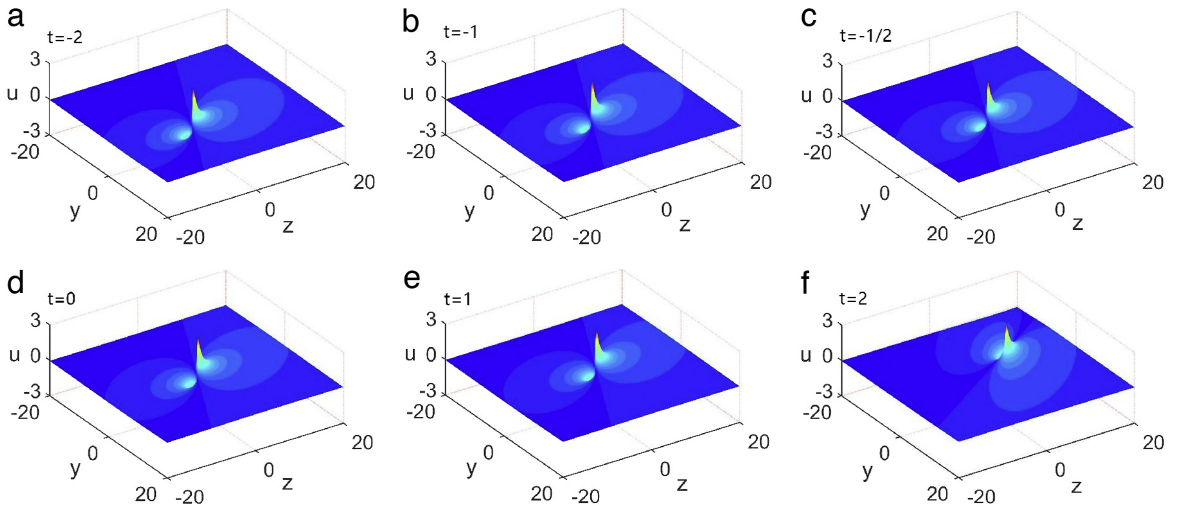

Fig. 13. The time evolution of lump solutions (23) of Eq. (1) in the (y, z) plane for parameters $p_1 = 1 - 2I,\ \ p_2 = 1 + 2I,\ \ q_1 = 2,\ \ q_2 = 2$ at $x = 0$.

References

[1] M.J. Ablowitz, P.A. Clarkson, Solitons, Nonlinear Evolution Equations and Inverse Scattering, Cambridge University Press, 1991.
[2] V.B. Matveev, M.A. Salle, Darboux Transformations and Solitons, Springer, 1991.
[3] C.H. Gu, H.S. Hu, Z.X. Zhou, Darboux Transformation in Soliton Theory and its Geometric Applications, Shanghai Scientific and Technical Publishers, Shanghai, 1999.
[4] J. Weiss, M. Tabor, G. Carnevale, The painleve property for partial differential equation, J. Math. Phys. 24 (1983) 522–526.
[5] G.Q. Xu, Painlevé classification of a generalized coupled Hirota system, Phys. Rev. E 74 (2006) 027602.
[6] R. Hirota, The Direct Method in Soliton Theory, Cambridge University Press, 2004.
[7] W.X. Ma, E.G. Fan, Linear superposition principle applying to Hirota bilinear equations, Comput. Math. Appl. 61 (2011) 950–959.
[8] C. Rogers, W.K. Schief, Bäcklund and Darboux Transformations: Geometry and Modern Applications in Soliton Theory, Cambridge University Press, 2002.
[9] P.J. Olver, P. Rosenau, The construction of special solutions to partial differential equations, Phys. Lett. A 114 (1986) 107–112.
[10] G.W. Bluman, A.F. Cheviakov, S.C. Anco, Applications of Symmetry Methods to Partial Differential Equations, Springer, New York, 2010.
[11] L.L. Huang, Y. Chen, Nonlocal symmetry and similarity reductions for the Drinfeld-Sokolov-Satsuma-Hirota system, Appl. Math. Lett. 64 (2017) 177–184.
[12] M. Tajiri, T. Arai, Growing-and-decaying mode solution to the Davey–Stewartson equation, Phys. Rev. E 60 (1999) 2297.
[13] N. Akhmediev, J.M. Soto-Crespo, A. Ankiewicz, How to excite a rogue wave, Phys. Rev. A 80 (2009) 043818.
[14] D.J. Kedziora, A. Ankiewicz, N. Akhmediev, Second-order nonlinear Schrödinger equation breather solutions in the degenerate and rogue wave limits, Phys. Rev. E 85 (2012) 066601.
[15] J.S. He, H.R. Zhang, L.H. Wang, A.S. Fokas, Generating mechanism for higher-order rogue waves, Phys. Rev. E 87 (2013) 052914.
[16] C. Liu, Z.Y. Yang, L.C. Zhao, W.L. Yang, Vector breathers and the inelastic interaction in a three-mode nonlinear optical fiber, Phys. Rev. A 89 (2014) 055803.
[17] J. Satsuma, M.J. Ablowitz, Two-dimensional lumps in nonlinear dispersive systems, J. Math. Phys. 20 (1979) 1496–1503.
[18] D.J. Kaup, The lump solutions and the Bäcklund transformation for the three-dimensional three-wave resonant interaction, J. Math. Phys. 22 (1981) 1176–1181.
[19] K. Imai, Dromion and lump solutions of the Ishimori-I equation, Progr. Theoret. Phys. 98 (1997) 1013–1023.
[20] W.X. Ma, Lump solutions to the Kadomtsev–Petviashvili equation, Phys. Lett. A 379 (2015) 1975–1978.
[21] J.Y. Yang, W.X. Ma, Z.Y. Qin, Lump and lump-soliton solutions to the (2+1)-dimensional Ito equation, Anal. Math. Phys. (2017). http://dx.doi.org/10.1007/s13324-017-0181-9.
[22] H.Q. Zhao, W.X. Ma, Mixed lump-kink solutions to the KP equation, Comput. Math. Appl. 74 (2017) 1399–1405.
[23] W.X. Ma, Lump-type solutions to the (3+1)-dimensional Jimbo–Miwa equation, Int. J. Nonlinear Sci. Numer. Simul. 17 (2016) 355–359.
[24] J.Y. Yang, W.X. Ma, Abundant lump-type solutions of the Jimbo–Miwa equation in (3+1)-dimensions, Comput. Math. Appl. 73 (2017) 220–225.
[25] D.H. Peregrine, Water waves, nonlinear Schrödinger equation and their solutions, J. Aust. Math. Soc. Ser. B 25 (1983) 16–43.
[26] N. Akhmediev, A. Ankiewicz, J.M. Sotocrespo, Rogue waves and rational solutions of the nonlinear Schrödinger equation, Phys. Rev. E 80 (2009) 026601.
[27] Y.V. Bludov, V.V. Konotop, N. Akhmediev, Vector rogue waves in binary mixtures of Bose–Einstein condensates, Eur. Phys. J. Spec. Top. 185 (2010) 169–180.
[28] B.L. Guo, L.M. Ling, Q.P. Liu, Nonlinear Schrödinger equation: generalized Darboux transformation and rogue wave solutions, Phys. Rev. E 85 (2012) 026607.
[29] X. Wang, Y.Q. Li, Y. Chen, Generalized Darboux transformation and localized waves in coupled Hirota equations, Wave Motion 51 (2014) 1149–1160.
[30] J.C. Chen, Y. Chen, B.F. Feng, K.-i. Maruno, Rational solutions to two- and one-dimensional multicomponent Yajima-Oikawa systems, Phys. Lett. A 379 (2015) 1510–1519.
[31] X. Wang, Y.Q. Li, F. Huang, Y. Chen, Rogue wave solutions of AB system, Commun. Nonlinear Sci. Numer. Simul. 20 (2015) 434–442.
[32] X. Wang, J.L. Cao, Y. Chen, Higher-order rogue wave solutions of the three-wave resonant interaction equation via the generalized Darboux transformation, Phys. Scr. 90 (2015) 105201.

[33] X.E. Zhang, Y. Chen, Rogue wave and a pair of resonance stripe solitons to a reduced (3+1)-dimensional Jimbo–Miwa equation, Commun. Nonlinear Sci. Numer. Simul. 52 (2017) 24–31.
[34] N. Akhmediev, A. Ankiewicz, M. Taki, Waves that appear from nowhere and disappear without a trace, Phys. Lett. A 373 (2009) 675–678.
[35] W.X. Ma, Y. Zhang, Y.N. Tang, J.Y. Tu, Hirota bilinear equations with linear subspaces of solutions, Appl. Math. Comput. 218 (2012) 7174–7183.
[36] L.N. Gao, X.Y. Zhao, Y.Y. Zi, J. Yu, X. Lü, Resonant behavior of multiple wave solutions to a Hirota bilinear equation, Comput. Math. Appl. 72 (2016) 1225–1229.
[37] X. Lü, W.X. Ma, Study of lump dynamics based on a dimensionally reduced Hirota bilinear equation, Nonlinear Dynam. 85 (2016) 1217–1222.
[38] L.N. Gao, Y.Y. Zi, Y.H. Yin, W.X. Ma, X. Lü, Bäcklund transformation, multiple wave solutions and lump solutions to a (3+ 1)-dimensional nonlinear evolution equation, Nonlinear Dynam. 89 (2017) 2233–2240.
[39] C.J. Wang, Lump solution and integrability for the associated Hirota bilinear equation, Nonlinear Dynam. 87 (2017) 2635–2642.
[40] C. Qian, J.G. Rao, Y.B. Liu, J.S. He, Rogue waves in the three-dimensional Kadomtsev–Petviashvili equation, Chin. Phys. Lett. 33 (2016) 110201.